EUROPEAN ORGANIZATION FOR NUCLEAR RESEARCH

CERN-EP/85-55
25 April 1985

A COMPARISON OF DIRECT PHOTON, π^0, AND η PRODUCTION IN $p\bar{p}$ AND pp INTERACTIONS AT THE CERN ISR

(The Axial Field Spectrometer Collaboration)

T. Åkesson[5], M.G. Albrow[11], S. Almehed[7], E. Anassontzis[1], R. Batley[5], O. Benary[12], H. Bø ggild[6], O. Botner[6], H. Breuker[5], H. Brody[8], V. Burkert[2], B. Callen[8], R. Carosi[5], A.A. Carter[10], J.R. Carter[4], P.C. Cecil[4], V. Chernyatin[14], Y. Choi[9], W.E. Cleland[9], S. Dagan[12], E. Dahl-Jensen[6], I. Dahl-Jensen[6], P. Dam[6], G. Damgaard[6], B. Dolgoshein[14], S. Eidelman[16], M.W. Evans[11], C.W. Fabjan[5], P. Frandsen[5], S. Frankel[8], W. Frati[8], I. Gavrilenko[15], M.D. Gibson[11], U. Goerlach[5], Y. Goloubkov[14], H. Gordon[3], K.H. Hansen[6], V. Hedberg[7], J.W. Hiddleston[11], J.E. Hooper[6], P. Ioannou[1], G. Jarlskog[7], P. Jeffreys[11], T. Jensen[5], A. Kalinovsky[14], V. Kantserov[14], S. Katsanevas[5], G. Kesseler[5], T. Killian[3], C. Kourkoumelis[1], R. Kroeger[9], K. Kulka[7], J. v.d. Lans[5], J. Lindsay[5], D. Lissauer[12], B. Lörstad[7], T. Ludlam[3], I. Mannelli[5], A. Markou[1], S. Mayburov[15], N.A. McCubbin[11], U. Mjörnmark[7], R. Møller[6], W. Molzon[8], P. Nevsky[14], B.S. Nielsen[5], L.H. Olsen[5], Y. Oren[12], R.B. Palmer[3], G. Piskounov[16], D.C. Rahm[3], L.K. Resvanis[1], E. Rosso[5], A. Rudge[5], J. Schukraft[5], A. Shmeleva[5], V. Sidorov[16], H. Specht[13], I. Stumer[3], M. Sullivan[9], J.A. Thompson[9], G. Thorstenson[7], P. Vasiliev[15], E. Vella[8], J. Williamson[11], W.J. Willis[5], M. Winik[3], W. Witzeling[5], C. Woody[3] and W.A. Zajc[8]

ABSTRACT

We have measured the production of direct photons, π^0 's, and η's in $p\bar{p}$ and pp collisions at $\sqrt{s}$ = 53 GeV in the range $2 \leq p_T \leq 6$ GeV/c for the central rapidity region $|y| \leq 0.4$. No statistically significant difference between $p\bar{p}$ and pp interactions is observed.

(Submitted to Physics Letters B)

1 University of Athens, Greece.
2 Physikalisches Institut, Univ. Bonn, Fed. Rep. Germany.
3 Brookhaven National Laboratory, Upton, NY, USA.
4 Cambridge University, Cambridge, UK.
5 CERN, Geneva, Switzerland.
6 Niels Bohr Institute, Univ. Copenhagen, Denmark.
7 University of Lund, Sweden.
8 University of Pennsylvania, Philadelphia, Pa., USA.
9 University of Pittsburgh, Pa., USA.
10 Queen Mary College, London, UK.
11 Rutherford Appleton Laboratory, Didcot, UK.
12 University of Tel Aviv, Israel.
13 Physikalisches Institut, Univ. of Heidelberg, Fed. Rep. Germany.
14 Moscow Physical Engineering Institute, Moscow, USSR.
15 Lebedev Institute, Moscow, USSR.
16 Novosibirsk Institute of Nuclear Physics, Novosibirsk, USSR.

1. INTRODUCTION

Since the discovery of direct photon production in pp collisions at the CERN Intersecting Storage Rings (ISR) [1] there has been increasing interest in the study of this process. Direct photons are clean probes of parton hard-scattering subprocesses since they do not undergo any fragmentation. In pp collisions their main origin is supposed to be the QCD gluon Compton process ($qg \rightarrow q\gamma$). Contributions from bremsstrahlung have been shown to be small [2]. The amplitude of the annihilation process ($q\bar{q} \rightarrow g\gamma$) can only be determined by comparing the photon production in antiparticle and particle beams.

The high luminosity of the two final ISR $p\bar{p}$ runs makes it possible to compare direct photon production in the deep-inelastic region ($p_T \geq 4$ GeV/c). QCD calculations [3–5] predict an increase of the γ/π^0 ratio with respect to the pp data since the annihilation process should become more and more dominant with increasing p_T.

At low p_T the background to direct photons is mainly due to π^0 and η decays into two photons in which only one is detected. For a comparison of the photon signal, these particle yields have to be measured in $p\bar{p}$ and pp collisions.

2. APPARATUS AND DATA ANALYSIS

The experiment was performed with the Axial Field Spectrometer (AFS) [6]. In its final configuration the central drift chamber was surrounded by a 2π uranium calorimeter, consisting of a 6 radiation lengths electromagnetic part and a 3.6 absorption lengths hadronic part. For the detection of photons, the AFS was equipped with two high-granularity sodium iodide (NaI) walls [7] covering a solid angle of twice 0.6 sr. Their arrangement (each wall consisting of 600 crystals in a 20 × 30 matrix) inside the uranium calorimeter, one towards (NaI wall 2) and one opposite (NaI wall 1) the centre-of-mass motion, is shown in fig.1. The front faces of the NaI crystals are 3.5 × 3.5 cm and their length (13.8 cm) corresponds to 5.3 radiation lengths. In combination with the two uranium sections, an overall energy resolution of 9–6% (σ/E) for electrons in the range 1–4 GeV was measured in a test beam. Because the NaI walls were inside a magnetic field of 3.5 kG, the light from the crystals was read out with vacuum photodiodes.

An inelastic collision was indicated either by a coincidence between two scintillation counters at forward angles (beam–beam counters) or by two or more hits in a hodoscope covering the central rapidity region (inner hodoscope). The photon trigger was performed in two steps: a pretrigger signal required the sum of all energy in the electromagnetic part of the uranium calorimeter behind the NaI wall to be above a given threshold. On a second level (600 ns later), discriminators investigated the energy deposition in the NaI wall localized in a 3.5° strip of constant azimuthal angle (corresponding to two adjacent rows of crystals). Thus the readout was triggered by one or more electromagnetic showers in either wall 1 or wall 2. The combined (sodium iodide plus uranium) trigger thresholds correspond to approximately 1.8 GeV and 2.4 GeV of localized electromagnetic energy during the two runs in 1982 and 1983, respectively.

The absolute detector calibration was achieved by measuring the energy deposition of minimum ionizing particles in individual crystals. Losses in efficiency were monitored by two ^{137}Cs radioactive sources. The detector electronics were frequently checked by feeding test pulses into the preamplifiers.

The $p\bar{p}$ data described here were taken at $\sqrt{s} = 53$ GeV in two periods of 12 days during December 1982 and 18 days in November/December 1983. To minimize systematic errors, the pp comparison data were recorded under identical trigger and apparatus conditions immediately before or after $p\bar{p}$ runs. The stored antiproton current was 5–10 mA and the proton current was ~ 15 A, resulting in luminosities of the order of 2–4 × 10^{28} cm^{-2} s^{-1} in intersection 8, which was equipped with superconducting low-beta quadrupoles. The instantaneous luminosity of the pp runs was higher by a factor of 100. The final data sample corresponds to 30 nb^{-1} in $p\bar{p}$ and to 70 nb^{-1} in pp runs.

For the analysis, the raw pulse heights were corrected for pedestal shifts and transformed to energy, using individual calibration factors (peaks from minimum ionizing particles) and ADC slopes (measured via test pulses). The raw data were then passed through a software filter that removed events below trigger threshold and asked for minimum energies in the NaI plus U calorimeter. Details are given in tables 1a and 1b.

The remaining events (35%) were processed through the standard AFS off-line program chain. This includes pattern recognition in the NaI detectors and the U calorimeter, and tracking plus vertex reconstruction for charged particles in the drift chamber. The NaI pattern recognition program groups neighbouring crystals which share energy, into clusters of energy corresponding to individual showers, using a 3 × 3 matrix. The position and energy of each individual shower are determined by use of a χ^2 minimization procedure, employing an average lateral shower shape which has been determined with the EGS [8] shower simulation program. If more than 15 MeV are detected in an adjacent crystal outside the 3 × 3 matrix the minimization procedure is performed, assuming two overlapping showers. This is necessary in order to resolve nearby showers originating, for example, from high-p_T π^0's.

In order to reduce background from cosmic rays and beam-gas interactions, events were rejected if no vertex from charged particles was found in the beam-crossing region. The timing of the inner hodoscope and the downstream scintillation counters was required to be consistent with a single interaction, allowing no second interaction within ±30 ns of the nominal event time. The remaining data sample contained 53,000 $p\bar{p}$ and 102,000 pp events.

The analysis was done separately for each of the NaI detectors, and the results were found to be consistent within statistical errors. The combined results are presented here.

3. π^0 AND η PRODUCTION

The π^0's and η's were identified as resolved pairs of photon showers. Each shower was required to have an energy above 250 MeV. To improve the background rejection, which was necessary for the antiproton data, additional cuts were applied:

i) showers with a track pointing towards them were not combined with others to form a π^0 or η—this cut removed 35% of background and less than 2% of the signal itself;

ii) no third shower above 180 MeV was tolerated in the event unless it was a charged particle as indicated by a track.

Figure 2 shows the two-photon mass spectrum for events that passed all selection criteria (from the 1983 $p\bar{p}$ run). The experimental mass resolution was σ_{π^0} = 15 MeV and σ_η = 60 MeV. The accepted mass range was $80 \leq m_{\gamma\gamma} \leq 190$ MeV for π^0's and $400 \leq m_{\gamma\gamma} \leq 700$ MeV for η's. The remaining background under the π^0 peak (approximately 8% at a p_T of 2 GeV/c decreasing to 5% at a p_T of 5 GeV/c) was interpolated between the left and right levels of the background and subtracted. Figure 3 shows the ratio $(L^{-1}\, dN/dp_T)_{p\bar{p}}/(L^{-1}dN/dp_T)_{pp}$. We find this ratio to be 0.95 ± 0.08 in the p_T range of 2 to 6 GeV/c in good agreement with ref. [9]. In the region of the η the mass distribution was fitted by a Gaussian peak plus a polynomial background. The background (35% at a p_T of 2.8 GeV/c and 25% at a p_T of 4 GeV/c) was determined from the fit and subtracted to give the true η signal. The observed η rate was corrected for the $\eta \rightarrow 2\gamma$ branching ratio. The relative π^0/η acceptance was calculated by a geometrical Monte Carlo program giving an acceptance ratio of 2.05 at $\langle p_T \rangle$ = 2.8 GeV/c and 1.55 at $\langle p_T \rangle$ = 4.0 GeV/c. The relative reconstruction efficiency was calculated using EGS-generated events that were passed through the same analysis chain as the real data. This factor was found to be consistent with 1 in the considered p_T range.The resulting η/π^0 ratio is shown in fig. 4. The average value is 0.55 ± 0.04, in good agreement with ref. [10]. We do not observe any difference in the production of π^0's and η's between $p\bar{p}$ and pp data. Numerical values and systematic errors are given in tables 2a, 2b, and 3.

4. DIRECT PHOTON PRODUCTION

The background for the detection of direct photons comes mainly from meson decays where one shower falls inside the detector and one is outside. At high p_T ($\geq$ 4 GeV/c), additional background is caused by merged π^0's, where the two showers are too close together to be resolved. Finally, there is a contribution from asymmetric decays, where one photon has a small energy and thus escapes the analysis cuts.

The selection criteria for single photons were as follows:

i) No track was allowed to point at the single-photon candidate. This cut removes electromagnetic showers originating from charged particles.

ii) No second shower above 180 MeV was tolerated in the event unless it was a charged particle as indicated by a track. It has been checked that the rejection of all events containing a second shower above 180 MeV does not change the result on the reported γ/π^0 ratio.

iii) A shower radius cut of 8–25 mm was applied. This cut has been optimized by Monte Carlo methods and by looking at the radius of showers originating from clean π^0's.

iv) The single-photon shower had to be inside a fiducial volume of the detector, excluding a 2 cm strip at the edge.

v) For the shower with the largest energy among all additional showers above 50 MeV, we checked that it did not combine with the single photon candidate to form a π^0. The total shower multiplicity was 2–4 before applying this final cut.

The selection criteria for π^0's included the cuts described in Section 3 with the additional requirement that both showers of the π^0 were within the above-defined fiducial volume of the detector.

Figure 5 shows the raw γ/π^0 ratio obtained. The dashed line is the result of a Monte Carlo background calculation. A signal for direct photon production is seen in $p\bar{p}$ and pp data for transverse momenta above 4 GeV/c. A statistically significant difference between production in $p\bar{p}$ and pp collisions is not visible.

5. MONTE CARLO CALCULATION FOR THE γ/π^0 BACKGROUND

The effects of the trigger threshold, the shower reconstruction algorithm, and of all the cuts applied in the data analysis have been studied by Monte Carlo methods. With the EGS code, which describes the development of electromagnetic showers, 20,000 events (6000 γ's, 14,000 π^0's) have been generated at suitably chosen discrete momenta between 0.5 and 9.0 GeV/c. The events cover the complete fiducial volume of the detector.

First the trigger probability was calculated for each event according to a software simulation of the effect of the trigger system using the experimentally determined profile of the discriminator thresholds. Thus a weight was assigned to each event. Afterwards, all cuts of the data analysis were applied to the Monte Carlo events in the same manner to study their effect on the data and to optimize the cuts. In this way it was possible to determine the reconstruction probability for γ's and π^0's as well as the probability to misidentify a π^0 as a single photon. All probabilities were normalized to the fiducial volume used in the analysis. Figure 6 compares the reconstruction probability for γ's and π^0's (both with and without the effect of the trigger threshold). In a similar way the quality of the energy reconstruction (linearity and resolution) was obtained. The non-linearity was found to be $\leq$ 1% and the resolution (σ/E) 9% to 5% for 2 to 8 GeV/c, respectively. These values were obtained by use of the standard pattern recognition program. A reasonable efficiency for resolving single photons from π^0 decays was found up to π^0 laboratory momenta of 8 GeV/c, as shown in fig. 6.

Possible differences in the energy scale between photons and π^0's have been studied as well, using the EGS-generated events. Because of the steeply falling p_T spectra, they are of major importance for the determination of the γ/π^0 ratio. These differences turned out to be less than 0.5%.

In a further step the geometrical acceptance and the effects of the kinematics and of the steep p_T spectrum were investigated with a second Monte Carlo program. The p_T dependence of the measured particle production yield [11] was parametrized by the form $p_T^{-8}\,(1 - x_T)^{11}$. Then γ, π^0, η, η', and ω were generated in the phase space relevant for our geometry. Using the suitably parametrized results of the analysis of the EGS events for the trigger and reconstruction efficiencies, the overall acceptances for γ's and π^0's were calculated. The background to the γ/π^0 ratio due to misidentified π^0's has two contributions. The first stems from all asymmetric decays or merged π^0's where both showers fall inside the fiducial volume. The second (geometrical) contribution to the background comes from cases where only one γ from neutral-meson decays falls inside the detector. To calculate this contribution, the exact form of which is sensitive to the γ and π^0 efficiencies shown in fig. 6, the γ inside the detector is treated as a single photon. Figure 7 shows the different contributions to the γ/π^0 background. Whereas below 4 GeV/c the geometrical component is the dominant source, at higher momenta the contribution of merging π^0's dominates as indicated in fig. 7. We estimate the systematic uncertainty of the background calculation as $\pm 5\%$ at higher p_T and (because of the sensitivity to the trigger threshold curves) as $\pm 10\%$ at lower p_T. Systematic uncertainties were determined by varying the assumed parametrizations within reasonable limits and observing the change in the expected γ/π^0 background.

After subtraction of background and correction for the relative efficiency and acceptance of single photons and π^0's, we obtain the corrected γ/π^0 ratio as given in table 4 and shown in fig. 8. For comparison, results from ref. [12] (pp, $\sqrt{s} = 53$ GeV) are also shown. The observed excess of single photons in $p\bar{p}$ collisions is well described by the recent QCD calculation [5].

6. CONCLUSIONS

A signal of direct photon production has been observed in $p\bar{p}$ interactions at $\sqrt{s} = 53$ GeV for p_T values above 4 GeV/c. A comparison with our pp data shows no statistically significant difference. The result is in agreement with QCD calculations, which include higher-order corrections to the leading log approximation. We find no indication of a strong enhancement in the production of direct photons due to annihilation processes below p_T values of 6 GeV/c. The π^0 and η yields, which determine the background to observed single photons, were found to be equal for $p\bar{p}$ and pp data.

Acknowledgements

We thank the staff of the CERN AA, PS, and ISR, whose dedicated efforts enabled the $p\bar{p}$ runs to be so successful. Support from the Research Councils in our home countries is gratefully acknowledged.

REFERENCES

[1] M. Diakonou et al., Phys. Lett. **87B** (1979) 292.
M. Diakonou et al., Phys. Lett. **91B** (1980) 296.
A.L.S. Angelis et al., Phys. Lett. **94B** (1980) 106.

[2] T. Åkesson et al., Phys. Lett. **123B** (1983) 367.
T. Åkesson et al., Phys. Lett. **118B** (1982) 178.
A.L.S. Angelis et al., Phys. Lett. **98B** (1981) 115.

[3] P. Aurenche et al., Phys. Lett. **140B** (1984) 87.

[4] A.P. Contogouris and M. Sanielevici, CERN TH.3656 (1983).

[5] O. Benary, E. Gotsman and D. Lissauer, Z. Phys. C **16** (1983) 211.

[6] H. Gordon et al., Nucl. Instrum. Methods **196** (1982) 303.
O. Botner et al., Nucl. Instrum. Methods **196** (1982) 314.
O. Botner et al., Nucl. Instrum. Methods **179** (1981) 45.

[7] R. Batley et al., A highly segmented NaI detector with vacuum photodiode readout for measuring electromagnetic showers at the CERN ISR, to be published in Nucl. Instrum. Methods (1985).

[8] R.L. Ford and W.R. Nelson, SLAC–210 (1978).

[9] A.L.S. Angelis et al., Phys. Lett. **118B** (1982) 217.

[10] C. Kourkoumelis et al., Phys. Lett. **84B** (1979) 277.

[11] F.W. Büsser et al., Nucl. Phys. **B106** (1976) 1.

[12] E. Anassontzis et al., Z. Phys. C **13** (1982) 277.

Table 1a
Run statistics

ISR run	$\int L\,dt\ (cm^{-2})^{a)}$	Trigger threshold (GeV)	Events on DST
316 pp	0.11×10^{34}	1.8	7052
317 $p\bar{p}$	0.71×10^{34}	1.8	22644
389 pp	5.01×10^{34}	2.4	70796
390 $p\bar{p}$	2.31×10^{34}	2.4	30512
391 pp	1.77×10^{34}	2.4	23838

a) Corresponding to the final DST data

Table 1b
Software energy thresholds (GeV)

	Run 316/317		Run 389/390/391	
	NaI 1	NaI 2	NaI 1	NaI 2
E_{tot} [a)]	1.20	1.50	1.30	1.60
E_{NaI}	0.75	0.85	0.75	0.95
$E_{UCAL\ em}$	0.20	0.28	0.45	0.55

a) Energy summed up as NaI + $UCAL_{em}$ + $UCAL_{had}$

Table 2a

π^0 cross-section ratio

p_T [GeV/c]	2.11	2.36	2.71	3.21	3.71	4.21	4.79	5.79
R_{π^0} ($p\bar{p}$/pp)	0.94 ±0.03	0.99 ±0.03	1.01 ±0.02	0.99 ±0.03	0.99 ±0.06	0.97 ±0.10	1.05 ±0.15	0.59 ±0.27

Table 2b

η/π^0 ratio

p_T [GeV/c]	2.8	4.0
η/π^0($p\bar{p}$)	0.52 ±0.03	0.59 ±0.08
η/π^0 (pp)	0.56 ±0.02	0.53 ±0.05

Table 3

Systematic errors (in %)

1) Uncertainty in absolute energy scale ($\Delta E/E$)	5
2) Total Monte Carlo efficiency, geometrical acceptance, reconstruction efficiency	10
3) Luminosity	5

Table 4

Corrected γ/π^0 ratio

p_T[GeV/c]	3.21	3.71	4.21	4.79	6.12
γ/π^0 ($p\bar{p}$)	0.00 ±0.01	0.05 ±0.02	0.06 ±0.03	0.11 ±0.05	0.29 ±0.17
γ/π^0 (pp)	−0.01 ±0.01	0.03 ±0.01	0.05 ±0.02	0.11 ±0.03	0.13 ±0.08

Figure captions

Fig. 1 : Experimental set-up as seen from above.

Fig. 2 : Two-photon mass spectrum after analysis cut. Data from 1983 $p\bar{p}$ run as measured with NaI wall 2; 2.5 GeV/c $< p_T <$ 3.5 GeV/c.

Fig. 3 : Ratio of π^0 production obtained in $p\bar{p}$ collisions to that obtained in pp collisions.

Fig. 4 : Corrected η/π^0 ratio versus p_T. Comparison of $p\bar{p}$ and pp data.

Fig. 5 : Observed γ/π^0 ratio in $p\bar{p}$ and pp. The dashed line is the sum over all background contributions.

Fig. 6 : Reconstruction probability for γ's and π^0's (with and without trigger threshold effects) for NaI wall 2 and thresholds from the 1983 run.

Fig. 7 : Contributions to γ/π^0 background.

Fig. 8 : γ/π^0 ratio for $p\bar{p}$ and pp data after background subtraction and correction for relative geometrical acceptance and reconstruction efficiency. For comparison we show also the pp data at 90°, $\sqrt{s}$ = 53 GeV, from ref. [12]. The dashed and solid lines are the QCD predictions for the γ/π^0 ratio in $p\bar{p}$ and pp interactions given in ref. [5] ($\sqrt{s}$ = 63 GeV).

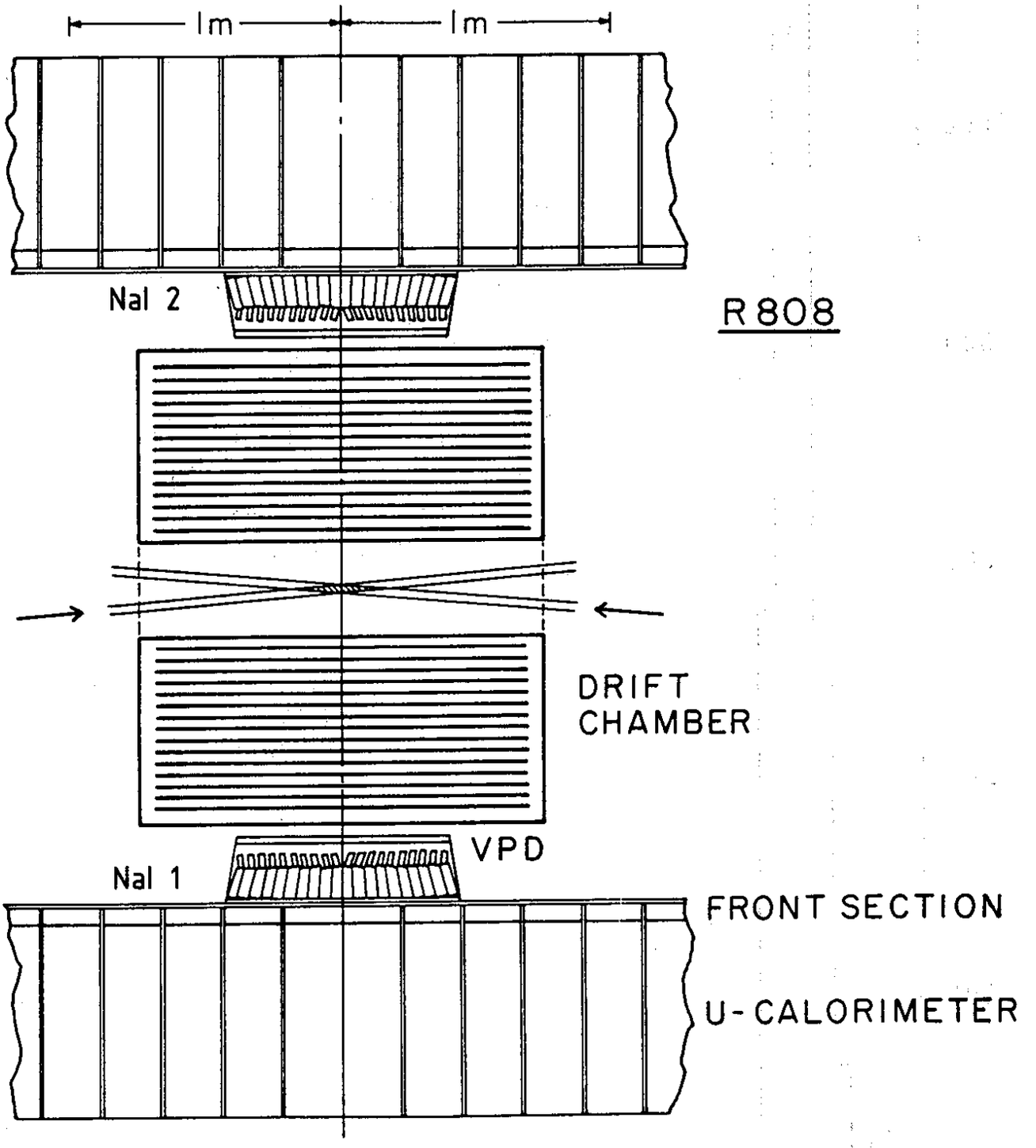
1m
1m
Nal 2
R808
DRIFT
CHAMBER
VPD
Nal 1
FRONT SECTION
U-CALORIMETER

Fig. 1

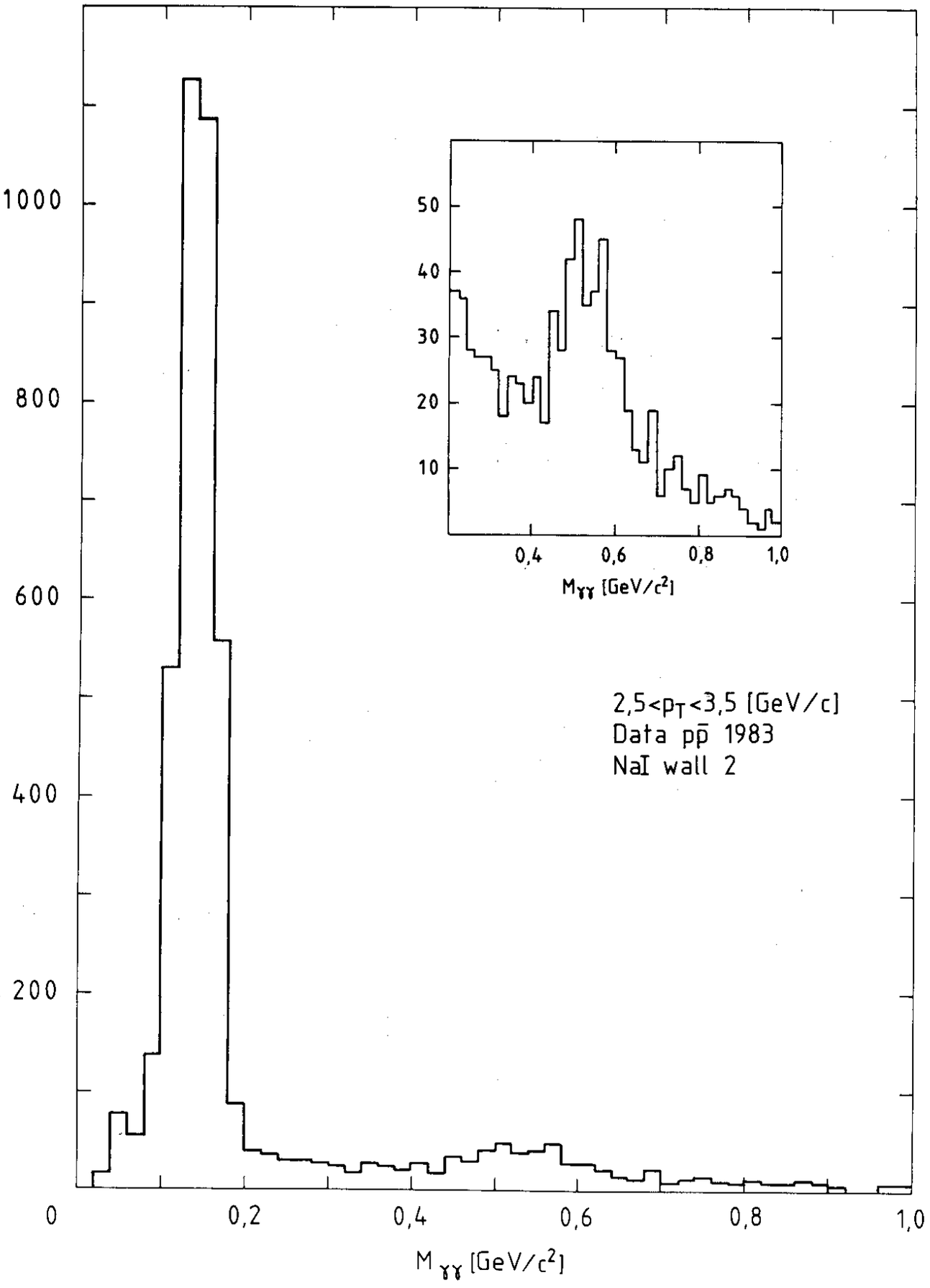
1000
800
600
400
200
0
0,2
0,4
0,6
0,8
1,0
M γγ [GeV/c²]
50
40
30
20
10
0,4
0,6
0,8
1,0
Mγγ [GeV/c²]
2,5<pT<3,5 [GeV/c]
Data pp̄ 1983
NaI wall 2

Fig. 2

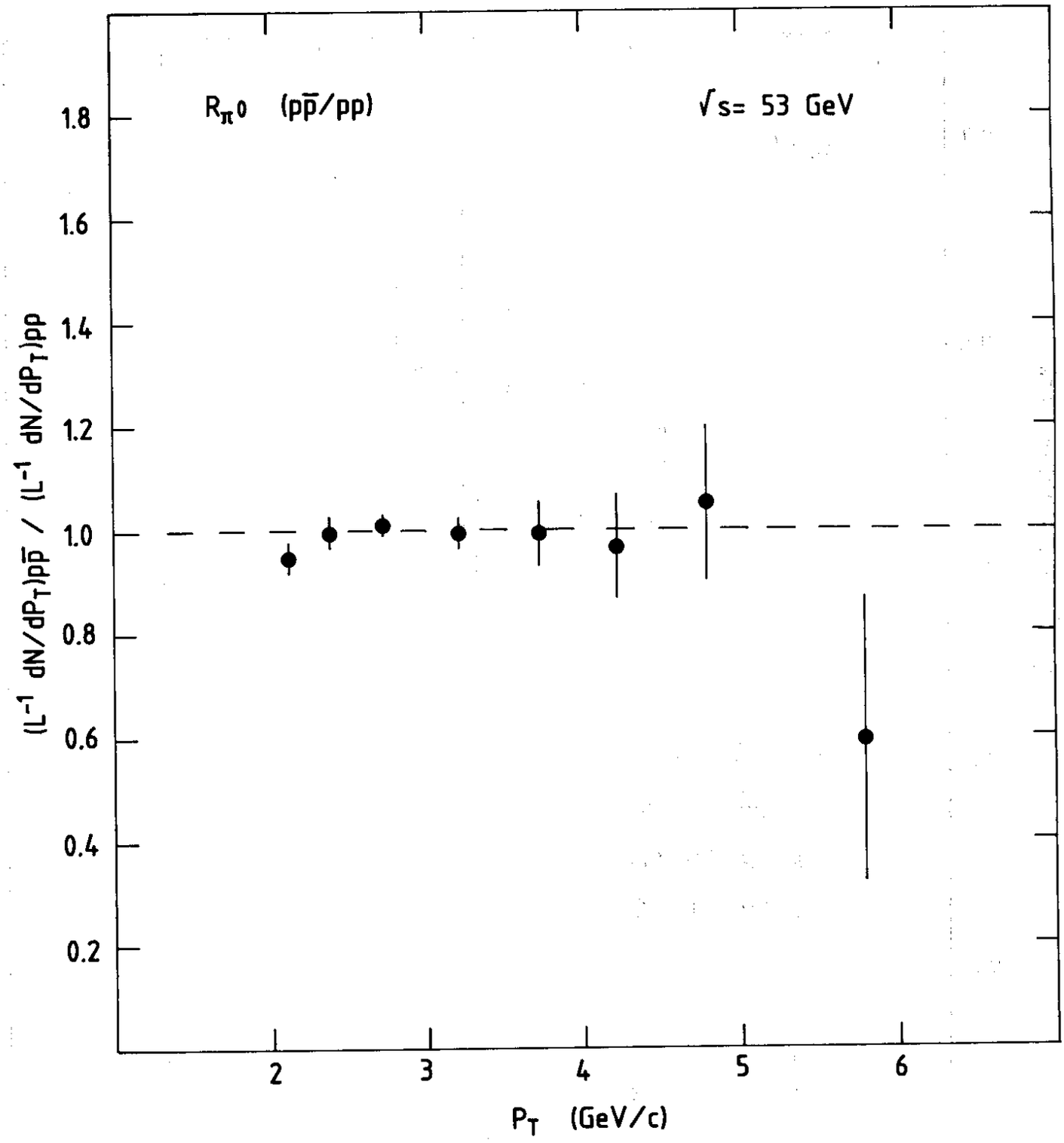
R_{π^0} $(p\bar{p}/pp)$
$\sqrt{s}$= 53 GeV
$(L^{-1}\ dN/dP_T)p\bar{p}\ /\ (L^{-1}\ dN/dP_T)pp$
1.8
1.6
1.4
1.2
1.0
0.8
0.6
0.4
0.2
2
3
4
5
6
P_T (GeV/c)

Fig. 3

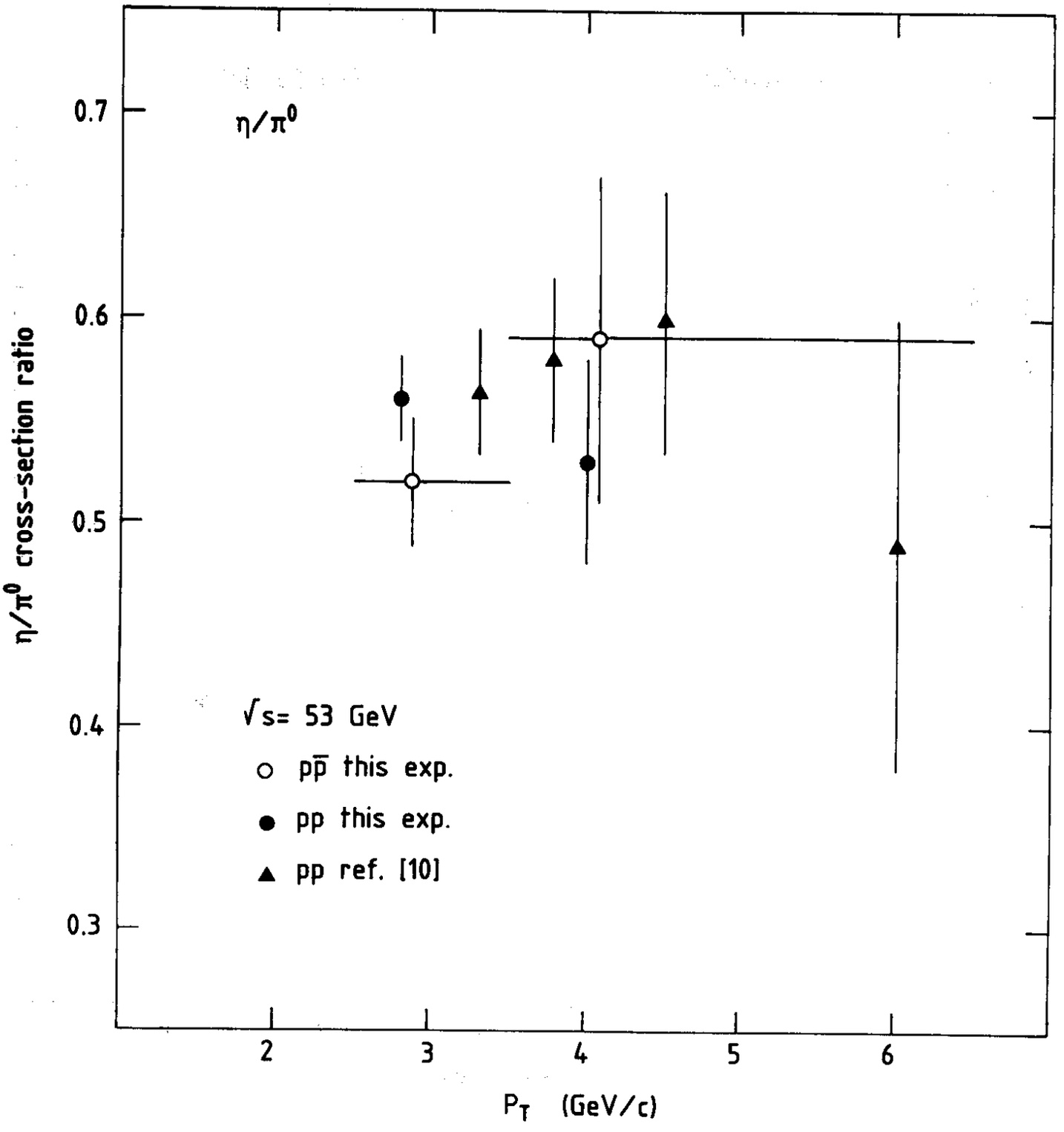
η/π⁰
η/π⁰ cross-section ratio
0.7
0.6
0.5
0.4
0.3
√s= 53 GeV
○ pp̄ this exp.
● pp this exp.
▲ pp ref. [10]
2
3
4
5
6
P_T (GeV/c)

Fig. 4

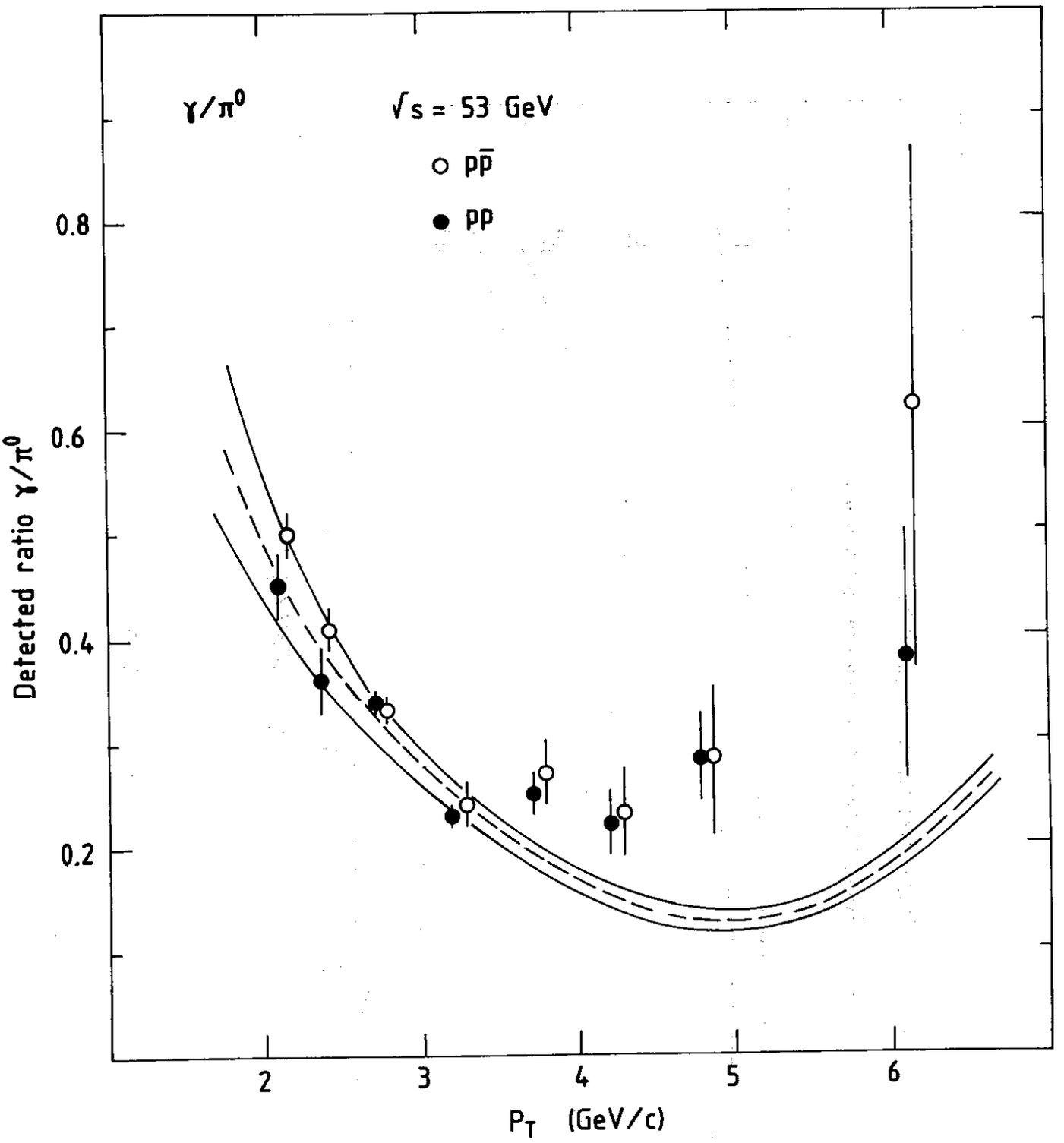

Fig. 5

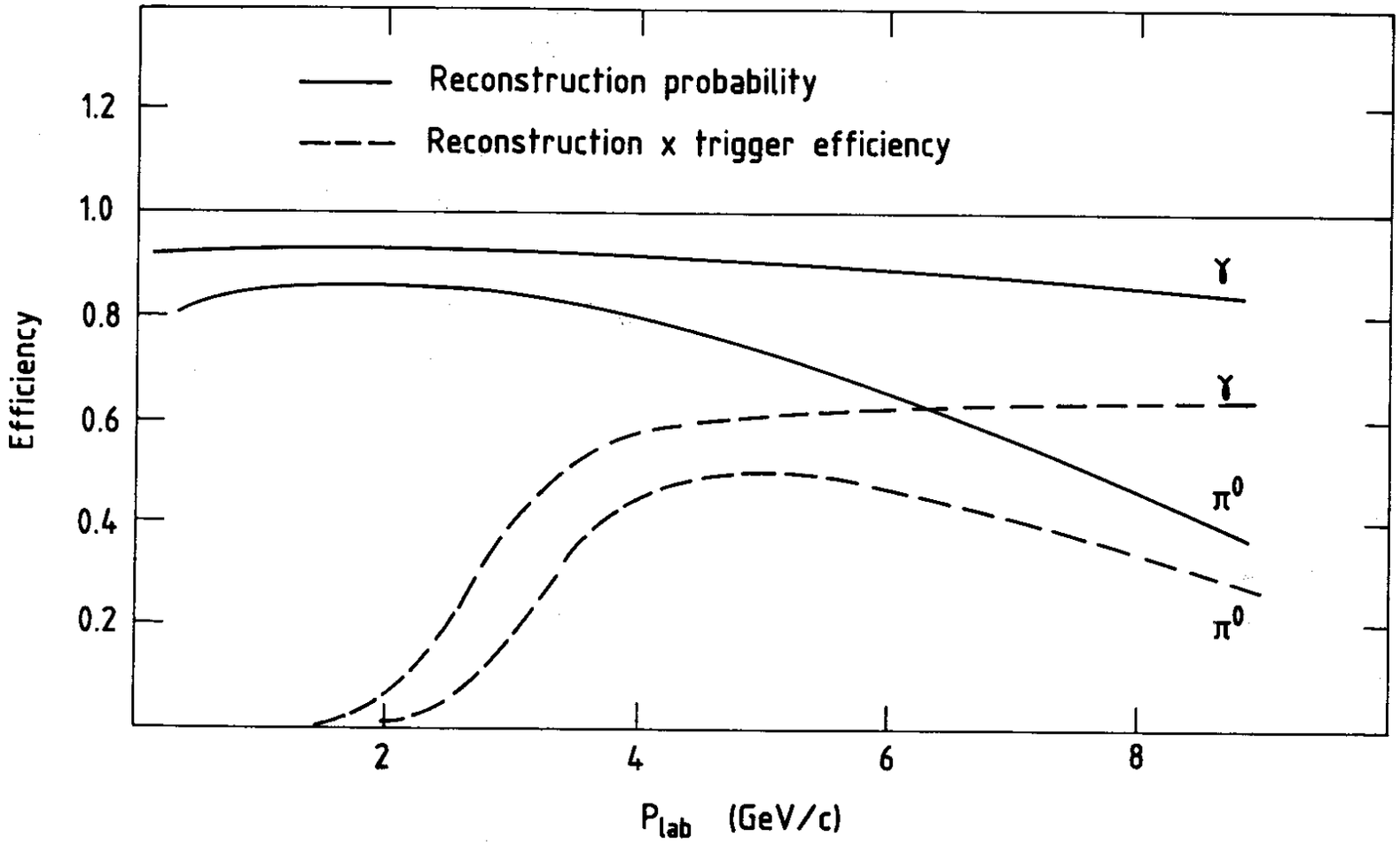
Reconstruction probability
Reconstruction x trigger efficiency
Efficiency
1.2
1.0
0.8
0.6
0.4
0.2
γ
γ
π0
π0
2
4
6
8
Plab (GeV/c)

Fig. 6

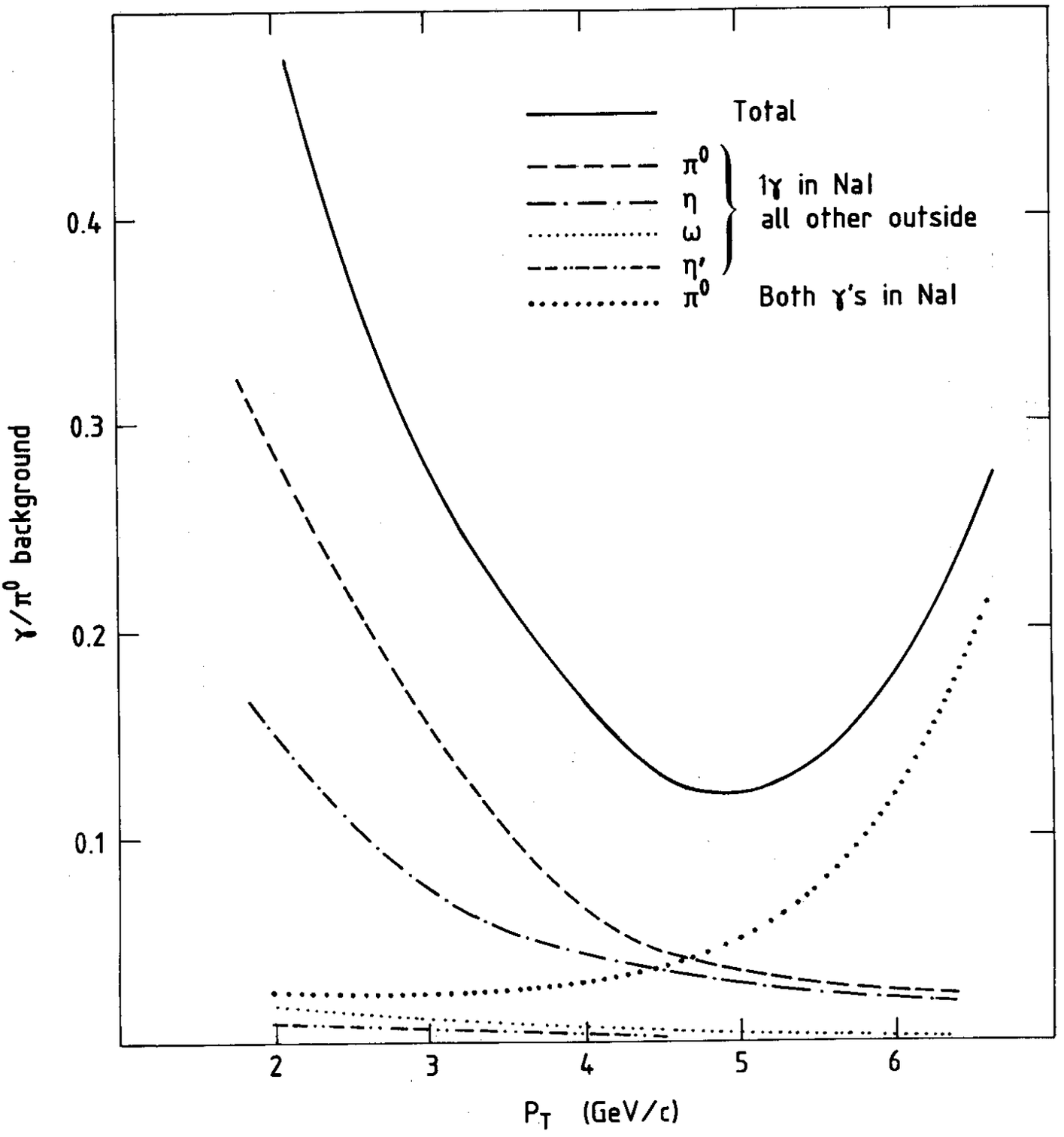
Total
π^0
η
ω
η'
1γ in NaI
all other outside
π^0
Both γ's in NaI
γ/π^0 background
0.4
0.3
0.2
0.1
2
3
4
5
6
P_T (GeV/c)

Fig. 7

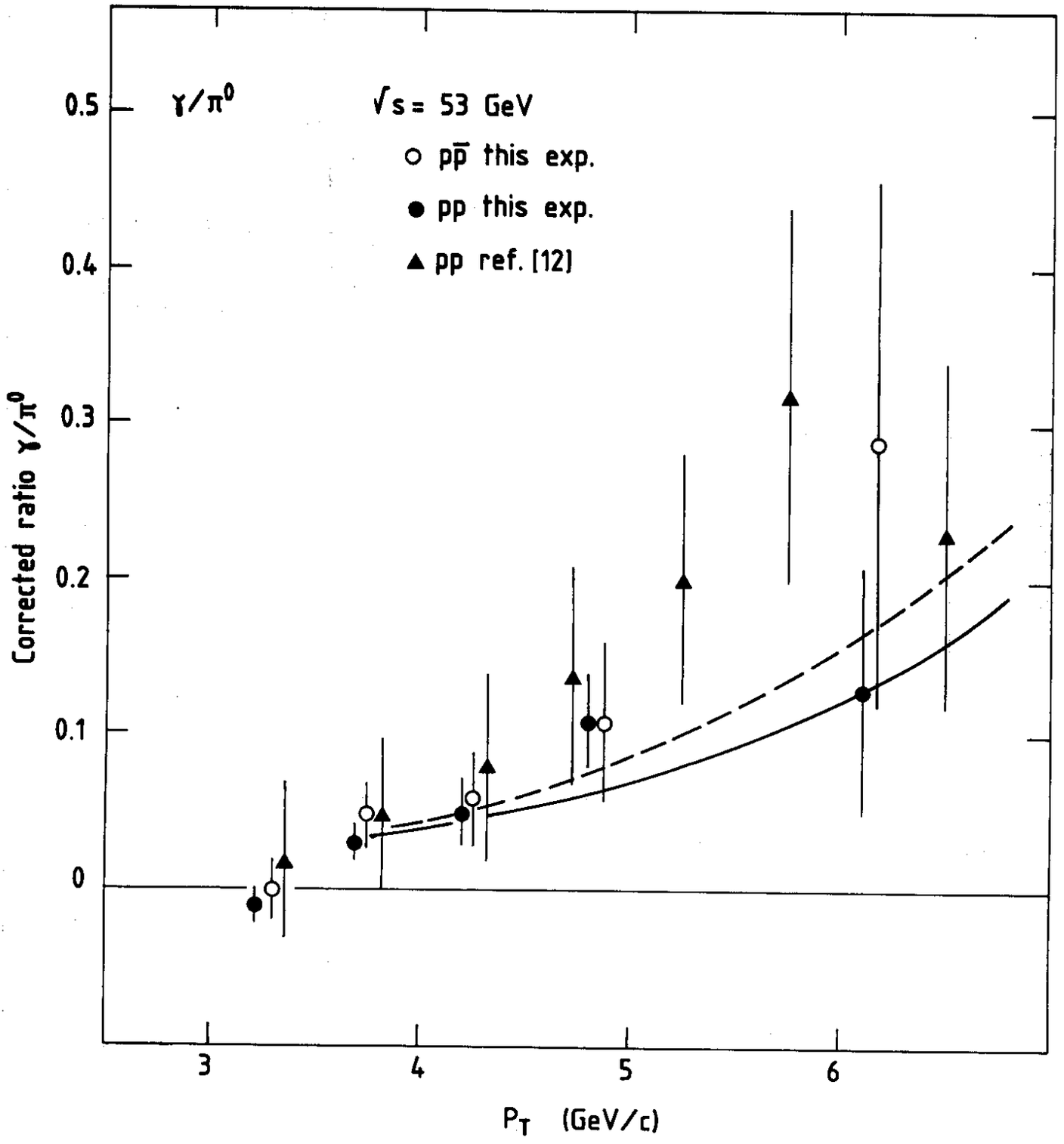
γ/π⁰
√s = 53 GeV
p$\bar{p}$ this exp.
pp this exp.
pp ref. [12]
Corrected ratio γ/π⁰
0.5
0.4
0.3
0.2
0.1
0
3
4
5
6
P_T (GeV/c)

Fig. 8